

Influence of PVA and CMC on the Properties of Pigment Coating Colors and their Effects on Curtain Stability

Eun Heui Choi, Chae Hoon Kim, Hye Joung Youn, and Hak Lae Lee*

The influence of polyvinyl alcohol (PVA) and carboxymethyl cellulose (CMC) on the properties of ground calcium carbonate (GCC) and clay coating colors, as well as its effect on curtain stability during the coating process was investigated. Based on the experimental results of the zeta potential, sediment porosity, rheological measurements, the floc formation mechanisms of the cobinders were proposed. The zeta potential decreased with an increase in the amount of added PVA, while it barely changed when CMC was added. This was attributed to the adsorption of PVA onto the pigment surface, while the adsorption of CMC was hindered by electrostatic repulsion. CMC cobinder increased the low-shear viscosity, but it resulted in relatively low viscosity under high-shear conditions, indicating the disruption of the formed flocs under high shear. The destabilization mechanism of the curtain coating differed depending on the type of cobinder. The PVA cobinder flocculates the coating color via a gelling mechanism, while the CMC cobinder flocculates the colors via a depletion flocculation mechanism.

Keywords: Curtain coating; GCC; clay; PVA; CMC; Curtain stability; Gelling; Depletion flocculation

Contact information: Department of Forest Sciences, Research Institute of Agriculture and Life Sciences, College of Agriculture and Life Sciences, Seoul National University, 151-921, Seoul, Rep. Korea;

*Corresponding author: lhakl@snu.ac.kr

INTRODUCTION

Curtain coating refers to a means of applying a premeasured sheet of coating colors that falls freely onto a substrate that is moving much faster than the curtain speed. The curtain coating technique has been used broadly for the production of chocolate-coated food products, photographic films, and specialty papers such as carbonless papers and thermal papers (Mendez and Morita 2001; Klass 2004) because it provides excellent coverage with uniformly thick coatings that are essential for these products (Trefz and Fröhlich 2005; Endres and Tietz 2007). The use of the curtain coating method for the production of pigment-coated papers, however, is quite recent, and more research is required to improve our understanding of this new technology.

Careful controls of coating color properties and processes are required for a curtain coating with pigment coating colors (Triantafillopoulos *et al.* 2004a). There are many challenges to achieve a successful curtain coating process, such as forming a uniform curtain with a high-solids pigment coating dispersion and applying it evenly onto a substrate that moves much faster than the curtain. The curtain coating, however, has many advantages as well. It allows coating at a high speed with high-solids colors. It also gives excellent runnability, owing to its non-contact nature. These are major reasons why many papermakers are interested in the curtain coating method. Many studies have been conducted on the effects of the coater design and the operating conditions on curtain coatings (Triantafillopoulos *et al.* 2004a, 2004b; Endres and Tietz 2007; Lee *et al.* 2012).

The first commercial curtain coating unit was installed at a linerboard mill in Korea, after which the benefits of producing coated linerboard by the curtain coating method was investigated by Lee *et al.* (2012) and Renvall *et al.* (2010). They showed that good coverage of the brown substrate is essential for the production of high-quality coated linerboard, and suggested that the strategic placement of pigments should be implemented for the most effective covering of the brown substrate. It has been suggested that the orientation of platy clay pigments would be more random in curtain-coated papers because there is no mechanical shearing action, as in the blade coating method (Klass 2004). Kim *et al.* (2013) determined the orientation of clay particles in curtain- and blade-coated papers and showed clearly that curtain coating produced a more random orientation of platy pigments, which resulted in higher porosity of the coating structure.

The running zone of a curtain coater can be divided into three zones; *i.e.*, the sheet-forming zone, the curtain-flow zone, and the impingement zone (Kistler 1983). In the sheet-forming zone, the coating color that is ejected uniformly from the curtain head creates a stable laminar flow. In the curtain-flow zone, the curtain stretches in the machine direction due to gravity. In the impingement zone the coating color impinges onto the substrate and is then stretched out following the substrate, which moves at a much higher speed. In each step of the curtain coating operation, careful control of the rheological property of the coating colors is needed to ensure a successful coating outcome (Triantafillopoulos *et al.* 2004a, 2004b).

It is important to expand our understanding of the relationship between the composition and properties of coating colors and the effects of the coating properties on the stability of the curtain. The effects of the pigment, latex binder and surfactant on the curtain coating have all been investigated (Urscheler *et al.* 2006; Renvall *et al.* 2009; Dahlvik *et al.* 2012; Lee *et al.* 2012).

However, the influence of cobinders such as polyvinyl alcohol (PVA) and carboxymethyl cellulose (CMC), which are widely used as rheology modifiers and water retention aids, has yet to be examined. The presence of water-soluble polymeric materials in aqueous coating colors would change not only the properties of the aqueous phase but also the interaction among solid particles. In this study, the influence of PVA and CMC on the rheological properties of curtain coating colors and their effects on the interactions of the pigment particles and the stability of the curtain were examined for clay and ground calcium carbonate base colors.

EXPERIMENTAL

Materials

Ground calcium carbonate (GCC; Setacarb 95K from Omya Korea) and kaolin clay (Hydragloss 90 from Huber) were used as coating pigments. The percentages of particles smaller than 2 μm contained in the GCC and clay were 96% and 99.5%, respectively. SB latex from Dow Chemical Co., Switzerland, specially prepared for curtain coatings, was used as a principal binder. The average particle size of the latex was 167 nm. The glass transition temperature of the latex was 20.7 $^{\circ}\text{C}$, the gel content was 67.5%, and the surface tension was 30.7 mN/m. Polyvinyl alcohol and carboxymethyl cellulose in powder forms obtained from Sigma Aldrich were used as cobinders. The molecular weight of the PVA was 13,000-23,000 g/mol and its degree of hydrolysis was 98%. The molecular weight and degree of substitution of the CMC were 90,000 g/mol and 0.7, respectively. Aqueous

solutions of PVA and CMC at 25% and 5%, respectively, were prepared and used in the experiment.

The GCC and clay dispersion were prepared. Twelve parts of SB latex were added as binder. PVA at five different addition levels of 0, 0.5, 1, 3, and 6 pph was used as a cobinder for the GCC- and clay-based coating colors. In addition, GCC- and clay-based coating colors containing CMC at five different dosage levels of 0, 0.1, 0.3, 0.5 and 1.0 pph were made and tested. The final solids content of the GCC coating colors was 60%, while that of the clay colors was 55%. Different solids levels were used to get the similar viscosities of coating colors without addition of cobinders. The pH of the coating colors was adjusted to 10.0 with a 1 N NaOH solution.

Methods

Zeta potential of pigment

The zeta potential of pigment in a coating color was measured using an electrophoretic light-scattering spectrophotometer (ELS-8000, Otsuka Electronics Co.). This instrument applies the laser Doppler principle to analyze the electric potential of a particle surface with a range of -100 to +100 mV. Coating colors were diluted with deionized water, and pH was adjusted to 10 with 1 M NaOH solution.

Sedimentation and porosity

To determine the coating porosity, centrifugation of the coating colors at 3000 G was carried out for 1.5 h. After decanting the supernatant, the weights of the coating sediment before and after drying were determined. The weight loss after drying was divided by the total volume of the sediment to calculate the porosity of the coating sediment.

Apparent viscosity and rheological property

To measure the low shear viscosity of coating colors, Brookfield viscometer (DV-II+Pro, Brookfield Engineering Laboratory, Inc.) was used. LV-1 spindle and the rotational speed of 100 rpm were employed. For the high shear viscosity determination, Hercules Hi-shear viscometer (DV-10, Kaltec Scientific, Inc.) was used. The shearing condition of 6600 rpm and 'E' bob were used. The viscoelastic properties were determined using a stress-controlled rotational rheometer (CVO, Bohlin Instruments). Complex modulus of coating color was determined over a frequency range of 0.16 to 16 Hz using a frequency sweep test. A cone-plate-type measuring device with a diameter of 40 mm and a cone angle of 2° was used for the viscoelastic characterization. All measurements were carried out at 23 °C. Pre-shearing was carried out for 1 min. to measure Brookfield viscosity. Other measurements were made without pre-shearing.

Surface tension

In the curtain coating operation, color curtain stretches under gravity at the curtain flow zone and creates large surface. Because fast stabilization of the expanded curtain surface is needed, dynamic surface tension at a low surface age is one of the most important parameters for stable curtain coating operation (Triantafillopoulos 2004a; Fröhlich and Tietz 2004; Bohnenkamp *et al.* 2005).

The static and dynamic surface tension levels were measured using static and bubble tensiometers (K12 and BP2, Krüss), respectively. After centrifuging the coating colors at 3000 G for 1.5 h, the supernatant was taken and used to measure the static and

dynamic surface tension at 23 °C. Platinum plate was used to measure the static surface tension according to Wilhelmy method. Dynamic surface tension for surface age of 100 to 50000 ms was measured using bubble pressure method.

Curtain stability

To examine the curtain stability, an experimental curtain coating head and circulation system were created. An image of the laboratory curtain coating head and a flow diagram of the experimental curtain unit are shown in Fig. 1. A sliding-type curtain head that forms a 150-mm-wide curtain was mounted on a steel frame. The coating color was supplied from the storage tank to the curtain head through a deaerator to remove the air entrained in the color.

The amount of coating color required to carry out the curtain stability experiment was 3.5 L. To hold the flow rate of the coating color to 1 L/min, a flow regulator was used. Two edge guides installed at both ends of the curtain sliding tip prevented the curtain from shrinking in width. While the upper ends of the edge guides were fixed, the lower ends of the guide could be widened with the use of a screw knob.

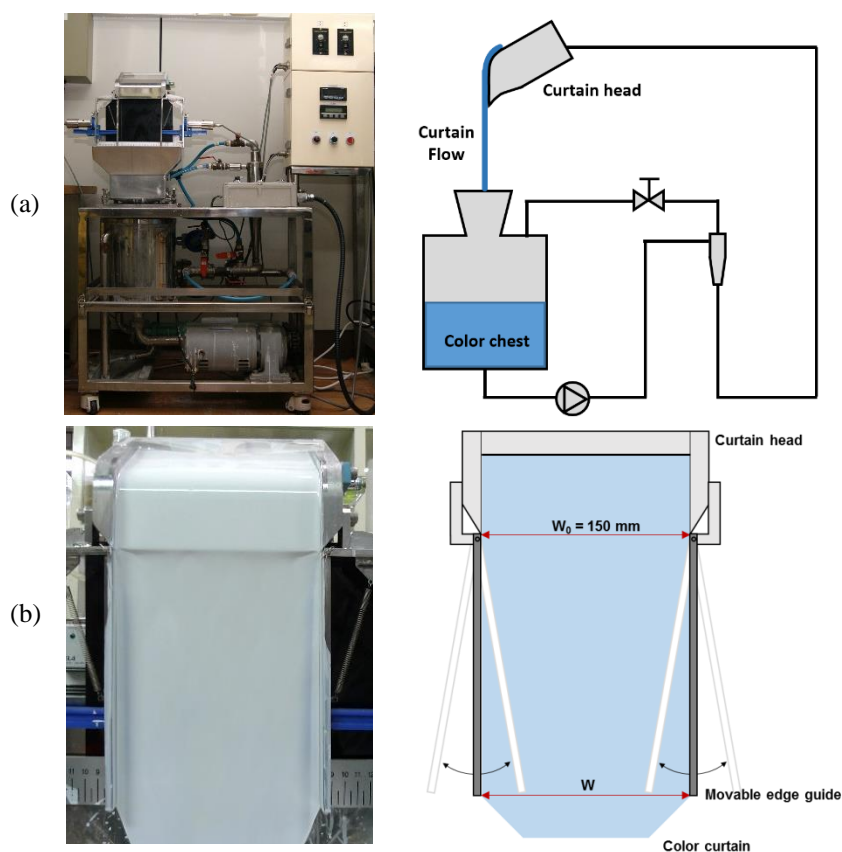


Fig. 1. Picture and schematic diagram of the curtain coating equipment: (a) and slide die of the curtain head: (b)

The width of the lower edge guides was increased until the curtain broke, and the width between the two lower edge guides at the moment this occurred was determined from video files recorded in front of the curtain head. From the width of the curtain at the moment it broke, W , and the initial width of the curtain, W_0 , which was 150 mm, the curtain

extension percentage that reflects the degree of curtain stability was calculated according to Eq. 1. The maximum curtain width was measured at least 5 times and average value of W was used.

$$\text{Curtain stability (\%)} = \frac{W}{W_0} \times 100 \quad (1)$$

RESULTS AND DISCUSSION

Zeta Potential

The zeta potentials of the GCC- and clay-based colors prepared without cobinders were -30.7 mV and -33.6 mV, respectively. The addition of PVA made the zeta potential less negative. The addition of CMC, however, did not cause a significant change in the zeta potential (Fig. 2). Earlier research found that PVA decreases the magnitude of the negative zeta potential (Işçi *et al.* 2006); this was attributed to the adsorption of PVA in thick layers on the surface, which will move the shear plane outwards from the particle surface (Sjöberg *et al.* 1999). Although nonionic PVA does not have any electrostatic attraction to clay or GCC surfaces, it adsorbs onto pigment surfaces via hydrogen bonding or entropy-driven adsorption (Theng 1982). This indicates that as more PVA is added, the adsorption of PVA, *i.e.*, the area of the pigment particles covered with PVA, increases. This also hides the negative charge on the pigment surface. In other words, the continuous increase in the zeta potential with the addition of PVA indicates that PVA molecules adsorb onto the surface and that the adsorption increases with the rate of addition.

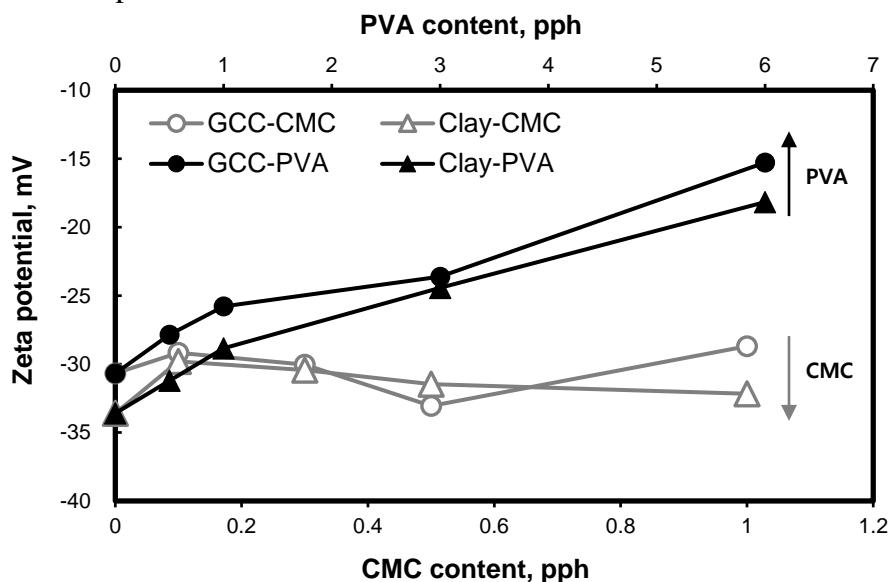


Fig. 2. Zeta potentials with increases in the PVA and CMC contents for GCC- and clay-based coating

On the other hand, the addition of CMC, which adsorbs little due to its negative charge, did not cause a significant change in the zeta potential. Highly negatively charged polymers such as sodium carboxymethyl cellulose polymers adsorb to a low extent on kaolin surfaces (Sjöberg *et al.* 1999). The adsorption of CMC on negatively charged

pigments has shown to be virtually negligible because the anionically charged dispersant molecules block the adsorption sites for CMC (Fadat *et al.* 1988).

Sedimentation and Coating Porosity

The centrifugation of the coating colors separated the coating colors into the sediment and the supernatant. The supernatants of both the GCC and the clay colors containing PVA cobinder were turbid irrespective of the PVA dosage, indicating that small pigment particles remained in the aqueous phase as stabilized discrete particles (Işçi *et al.* 2006). On the other hand, the supernatants of both the GCC and clay colors containing 0.5 pph and 1 pph of CMC cobinder, respectively, were clear, showing that all pigment particles settled down as sediment. This suggests that even small coating pigments tend to flocculate when the CMC addition rate exceeds a certain level.

The porosity of the GCC and clay color sediments containing PVA and CMC is depicted in Fig. 3. In general, the porosity of the coating sediment increased as more PVA or CMC was added, which indicated that coating components tend to form larger and more porous flocs with the increased addition of a cobinder. Al-Turaif *et al.* (2002) showed that the addition of CMC generates a coating with higher voids and lower gloss for both clay and PCC colors. The use of an associative thickener that interacts with the pigment particles and some coating components can create a network in the aqueous suspension (Nisogi *et al.* 2000). It is interesting to note that the porosity of the GCC colors was lower when PVA was used as a cobinder as compared to CMC.

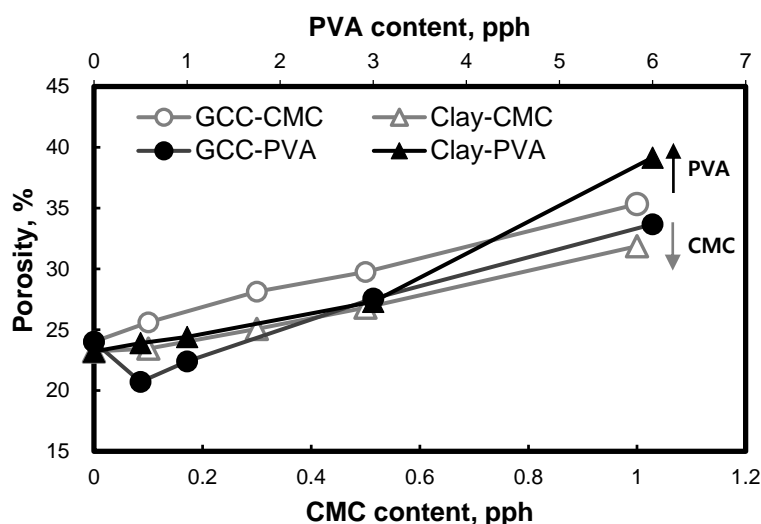


Fig. 3. Porosity vs. PVA and CMC additions for clay and GCC colors

On the other hand, the porosity of the clay colors increased substantially at a high PVA addition rate. This suggests that GCC gave more compact flocs when PVA was used, while clay formed tighter flocs when CMC was used. It is also notable that the addition of 0.5 pph or 1 pph of PVA decreased the porosity of GCC colors until it was below the porosity of the GCC color without PVA, which indicated that a more compact sediment was created at these dosage levels of PVA.

Surface Tension

Results for the static surface tension of CMC and PVA added coating colors are listed in Table 1. The static surface tension was quite low and did not show much variation upon additions of CMC and PVA. For the GCC colors, it ranged from 25.8 - 26.4 mN/m, and for the clay colors, it ranged from 26.8 to 27.1 mN/m.

Table 1. Static Surface Tension of Coating Colors

Pigment	Cobinder									
	PVA					CMC				
	0 pph	0.5 pph	1 pph	3 pph	6 pph	0 pph	0.1 pph	0.3 pph	0.5 pph	1 pph
GCC	26.2	26.4	26.4	26.0	- ¹⁾	26.2	26.3	26.2	26.1	25.8
Clay	27.1	27.1	27.0	26.8	26.9	27.1	27.0	27.1	26.7	26.9

Unit: mN/m

1) Static surface tension of GCC coating colors with 6 pph of PVA was not able to be measured due to high viscosity of color supernatant.

The dynamic surface tension measured with a bubble pressure tensiometer is depicted as a function of the surface age in Fig. 4. The dynamic surface tension increased when the surface age decreased. This indicated that it took time for the dissolved surfactant to move to the newly formed air bubble surface. One may speculate that an addition of polymeric water-soluble cobinders would hamper the movement of surfactant molecules.

The addition of cobinders increased the dynamic surface tension, but the increase was not as large except when more than 3 pph of PVA was used as a cobinder. These low dynamic surface tension seemed to be contributed by a significant amount of surfactant molecules in the aqueous phase of colors. This shows that the use of a cobinder did not have a substantially negative effect on the dynamic surface tension unless an excessive amount of PVA was used.

Apparent Viscosity and Rheological Properties

The viscosity levels of the coating colors containing either PVA or CMC are shown in Table 2.

Table 2. Low and High Shear Viscosity of the GCC and Clay Coating Colors

Pigment	Viscosity (cPs)	Cobinder									
		PVA					CMC				
		0 pph	0.5 pph	1 pph	3 pph	6 pph	0 pph	0.1 pph	0.3 pph	0.5 pph	1 pph
GCC	Low shear ¹⁾	44.8	141.6	171.6	370.7	832.6	44.8	186.9	776.2	1117.0	2250.0
	High shear ²⁾	11.9	13.2	14.9	20.9	36.4	11.9	13.6	15.9	16.0	20.2
Clay	Low shear ¹⁾	213.6	212.7	271.1	658.7	1866.0	213.6	331.1	535.1	782.2	1836.0
	High shear ²⁾	8.3	11.7	13.0	19.3	25.9	8.3	9.7	11.5	14.6	19.4

1) Low shear viscosity was measured using Brookfield viscometer

2) High shear viscosity was measured using Hercules Hi-shear viscometer

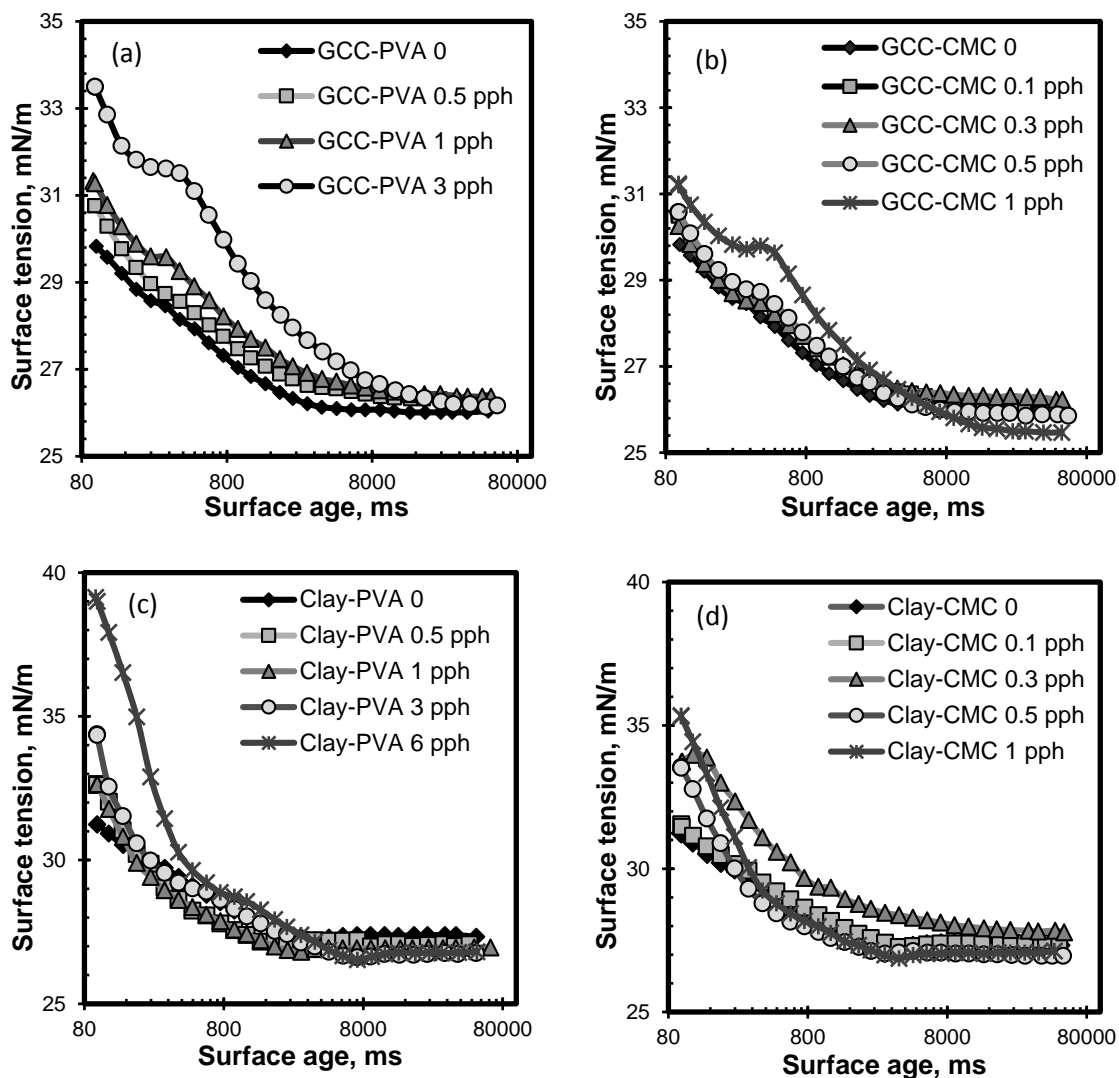


Fig. 4. Dynamic surface tension of GCC-PVA: (a), GCC-CMC (b), clay-PVA (c) and clay-CMC (d) colors measured with a bubble pressure tensiometer as a function of the surface age

The low and high shear viscosity comparison of the clay and GCC colors showed that clay colors gave a higher Brookfield viscosity than GCC colors, despite the fact that the solids content of the clay colors was 5% lower than that of the GCC colors. On the other hand, the clay colors showed lower viscosity under a high-shear condition. This was attributed to the platy particle shape of the clay, which tends to align to the shearing directions under high shear.

A comparison of the Brookfield viscosity data for colors containing 0.5 pph and 1.0 pph of PVA and CMC showed that CMC gave a much higher Brookfield viscosity than PVA for both the GCC and clay colors. The Hercules viscosities of CMC containing colors were also higher than those of the PVA colors, but the difference was not as great as it was with the Brookfield viscosity. This suggests that the flocculated pigment particles were redispersed again under high-shear conditions (Sandas and Salminen 1991).

While the Brookfield viscosities of the CMC coating colors were substantially higher than those of the PVA colors, the Hercules viscosities of the CMC coating colors were not as high compared to those of the PVA colors. This indicates that CMC coatings have a structure that breaks down rather easily under high-shear conditions as compared to PVA colors. In other words, CMC colors form greater interparticle networks under low-shear conditions, but they tend to be disrupted at high shear rates. On the other hand, PVA coating colors have structural characteristics that persist and withstand high shear forces. This explains why shear-thinning was more pronounced in the CMC coating colors than in the PVA colors. Sandas and Salminen (1991) showed that the rheology reflects the differences in the shear resistance of the aggregates formed via the interaction of each pigment-cobinder combination.

The viscoelastic properties of the coatings, which provide information on the aggregation within the coating (Sandas and Salminen 1991; Nisogi *et al.* 2000), was determined. The loss modulus (G'') was considerably lower than the storage modulus (G') for all coating colors, which indicates that the colors had more of elastic than viscous characteristics throughout the whole frequency range investigated. The complex modulus (G^*), which shows a tendency similar to that of the storage modulus, is depicted in Fig. 5.

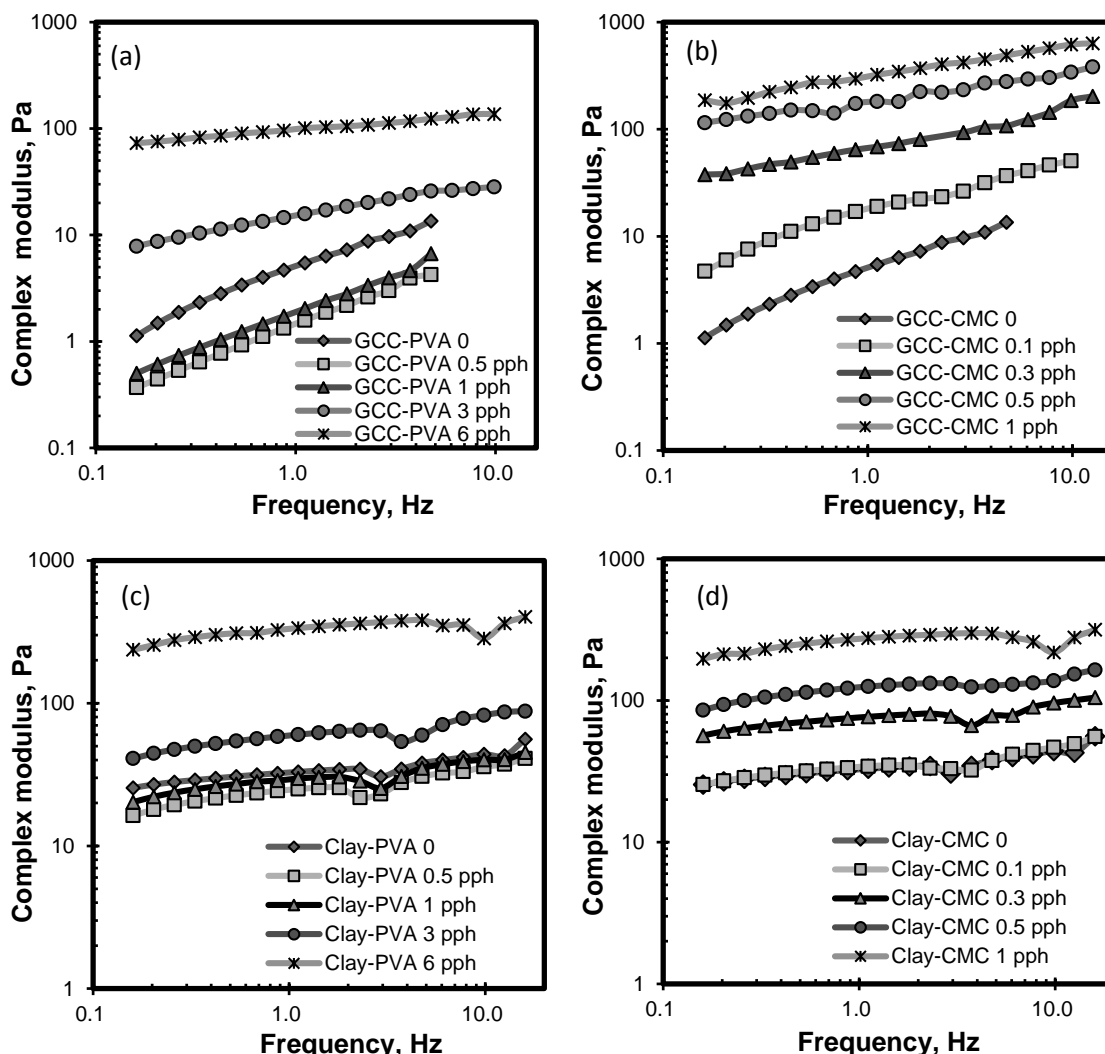


Fig. 5. Complex modulus of GCC-PVA: (a), GCC-CMC (b), clay-PVA (c) and clay-CMC coating colors as a function of the frequency at 0.16-16 Hz

The complex moduli of both the GCC and clay colors with small amounts of PVA were lower than those of the colors without PVA. Especially in the case of the GCC colors, a substantial reduction was observed. This was in good agreement with the lower porosity of the GCC coatings (Fig. 3). With a greater PVA addition, however, the complex moduli increased well above the case of no PVA addition. This suggests that the coatings start to show high elasticity at high addition rates, most likely due to the gelling of the coating pigments by the PVA. In other words, well-dispersed coating colors give a low complex modulus, while aggregated coatings tend to give a high complex modulus.

The results from the viscoelastic, viscosity, and coating porosity measurements indicate that PVA coating colors became well dispersed when small amounts of PVA were used as a cobinder. Well-dispersed coating colors give low Brookfield viscosity and low porosity levels (Lepoutre 1989). When the amount of PVA cobinder is increased to 3 pph or higher, gelling of the coating components by PVA molecules occurs, which increases the low shear viscosity, the complex moduli, and the coating porosity. However, small pigment particles remain in the aqueous phase because gelling does not flocculate all of the pigment particles.

For the CMC coating colors, the complex modulus increased with the CMC content. Colors containing the CMC cobinder did not show a lower complex modulus than the control, which suggests that the CMC increased the interaction among the pigment particles, even at low addition rates. Because the zeta potential measurement indicated that CMC does not adsorb onto GCC or clay, CMC dissolved in the aqueous phase caused flocculation of the color components not by gelling or bridging but by a depletion mechanism (Fadat *et al.* 1988; Whalen-Shaw and Gautam 1990).

Mechanism

In general, an aqueous colloidal system is stabilized by electrostatic repulsion due to coulombic forces, steric repulsion from the adsorbed polymeric layer of the cobinder, and electrosteric repulsion due to the adsorbed layer of the polyelectrolyte (Tadros 2007). Depletion forces due to non-adsorbing polymeric cobinder species cause floc formation (Tadros 1996). The colloidal stability of coating colors is usually determined by a combination of the above forces. Depending on the type and addition level of the cobinder, the means of stabilizing an aqueous coating system will differ. Based on the experimental data on the zeta potential, the porosity, and the rheological properties of coatings, the mechanisms of stabilization and destabilization for GCC and clay coatings with PVA and CMC as cobinders are derived. These are depicted in Figs. 6 and 7.

For the GCC colors, when the addition rate of PVA is less than 1 pph, PVA adsorbs onto the GCC surface and disperses the pigment particles owing to its protective colloidal effect (Fig. 6 (a)). This results in a lower zeta potential, porosity, and complex moduli of this coating color. When the addition rate is greater than 3 pph, PVA molecules start to form a network of GCC particles that have some resistance against disruption by shear forces because the PVA molecules become entangled with each other at high dosages. Moreover, this entanglement of PVA interconnects the GCC particles and causes the gelling of the coating materials (Fig. 6 (b)).

When 0.1 pph of CMC was used as a cobinder, no significant change occurred in the GCC colors (Fig. 6 (c)). However, at a higher dosage, CMC caused flocculation of GCC pigments via a depletion mechanism (Fig. 6 (d)). All GCC particles irrespective of the particle size flocculated via this depletion flocculation; thus, a clear supernatant was obtained along with high porosity of the coating at a high CMC dosage. The fact that GCC-

CMC colors resulted in high viscosity at a low shear level and low viscosity under high shear indicates that the flocs formed via the depletion flocculation of GCC have low tenacity against disruptions by shear, most likely because no entanglement of the polymers is involved in the depletion flocculation mechanism and because the shape of the GCC particles is not suitable for depletion flocculation.

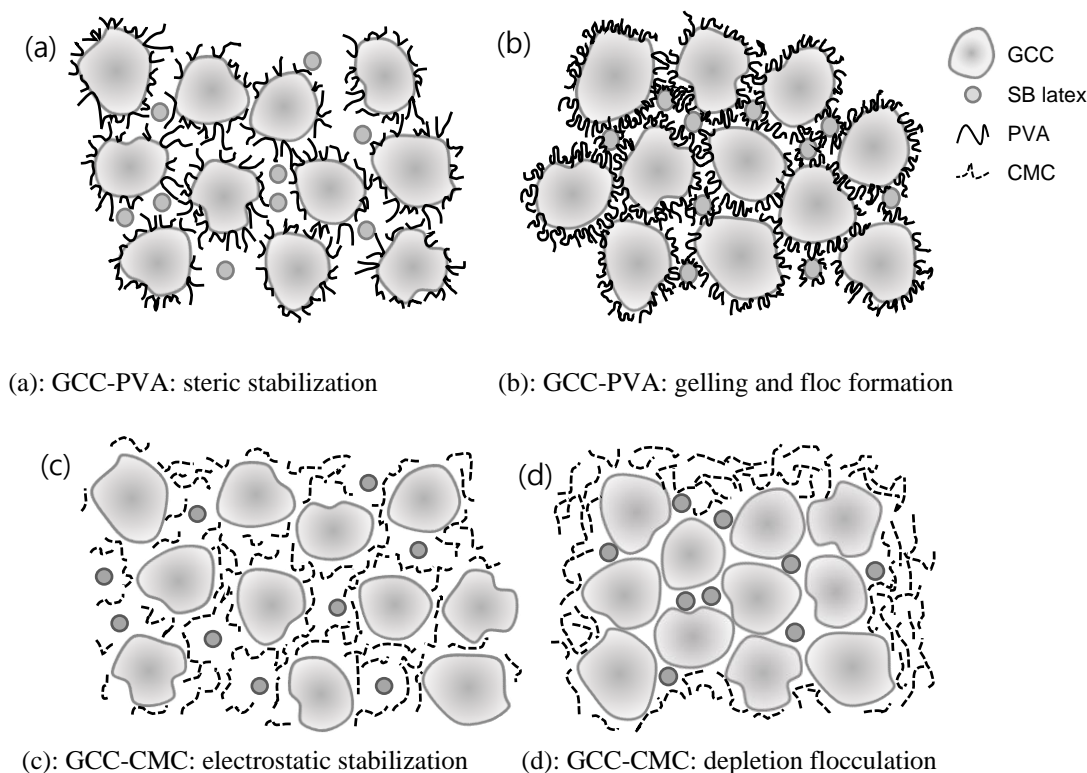


Fig. 6. Mechanism of the stabilization and destabilization of GCC coatings with PVA and CMC cobinders

The suggested mechanism influencing the interaction between PVA and CMC cobinders for clay-based coating colors is depicted in Figs. 7 (a)-(d). Essentially, the action of both cobinders appears similar to that in the GCC case. Interparticle interaction for depletion flocculation, however, seems to take place differently from the GCC case owing to the differences in the pigment shape (Sjöberg 1999). The dispersibility of clay coating colors was improved due to steric stabilization caused by the adsorbed PVA when a small amount of PVA was added (Fig. 7(a)). This contributed to stable Brookfield viscosity and stable coating porosity. A further increase in the amount of PVA added caused the Brookfield viscosity and porosity to increase rapidly due to the formation of highly porous flocs (Fig. 7(b)). However, it is interesting to note that the high shear viscosity of clay colors containing PVA as a cobinder was lower than that of the GCC-PVA color. This was attributed to the loose structure of the clay flocs, which are formed by clay particles arranged randomly in a loose arrangement. Platy particles held together by PVA molecules in a random arrangement would easily erode from the surface or become disrupted under a high-shear condition.

When the addition rate exceeds 0.3 pph, depletion flocculation of clay particles occurs; this is reflected in the increased porosity, the low shear viscosity, and the high

complex moduli. Depletion flocculation occurs when macromolecules are excluded from the interparticle region, as their insertion into such a restricted space would otherwise give rise to a loss of configurational entropy, resulting in a free-energy increase (Fadat *et al.* 1988; Tadros 1996). Because depletion flocculation requires a close approach of particles, clay plates appear to approach each other in a parallel arrangement, as shown in Fig. 7 (d).

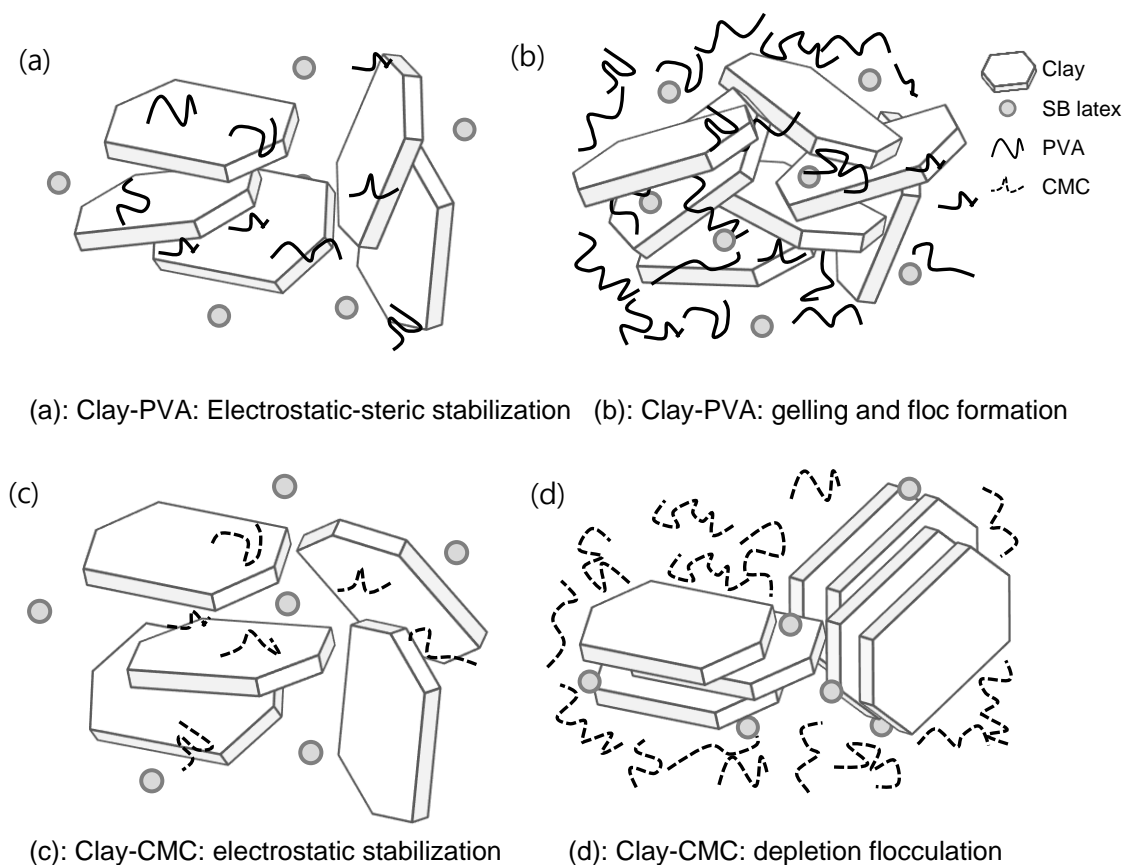


Fig. 7. Mechanism of the stabilization and destabilization of GCC coatings with PVA and CMC cobinders

Curtain Stability

The curtain stability levels of the coating colors are depicted in Fig. 8. When the addition of a cobinder improved the coating dispersion, *e.g.*, when PVA was added at a low dosage, the stability of the curtain was improved. A greater addition of PVA, however, significantly reduced the curtain stability due to the gelling of the coating components. Upon the addition of CMC addition, no improvement of the curtain stability was observed. A substantial reduction of the curtain stability was observed for clay-CMC coatings, most likely because depletion flocculation occurs most strongly for platy clay pigments. For the GCC coatings, no reduction in the curtain stability was observed at a 0.1 pph addition rate of CMC, in all probability due to the less effective depletion flocculation for the irregularly shaped GCC particles. The contraction of the curtain film is associated with a low color flow rate and high color elasticity (Trefz and Fröhlich 2005; Urscheler *et al.* 2006). Considering that the flow rate of the curtain was kept constant at 1 L/min, increases in the coating elasticity influenced the degree of curtain stability as well.

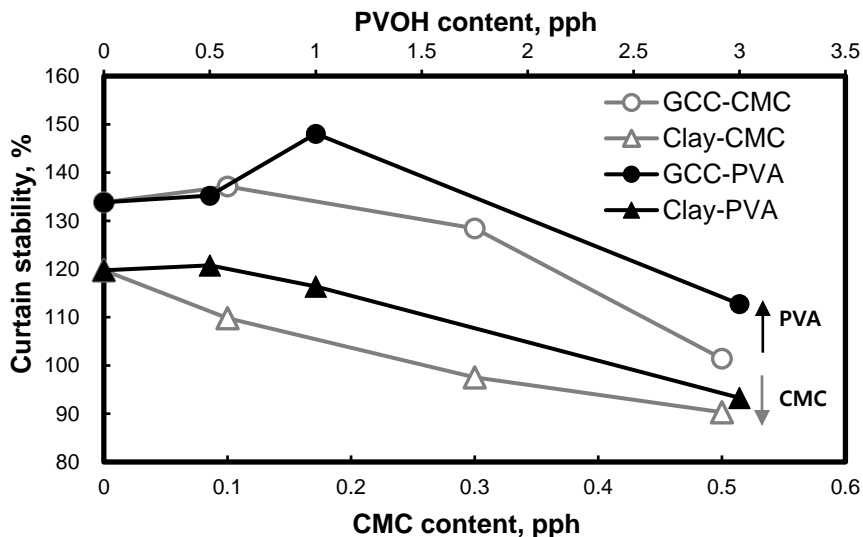


Fig. 8. Curtain stability with an increase in the PVA content of the clay-based coating colors

CONCLUSIONS

1. An addition of PVA caused a decrease in the zeta potential, whereas an addition of CMC did not have a significant effect. This was attributed to the adsorption of PVA onto the pigment particles and the non-adsorbing property of CMC.
2. When PVA was added at low levels, the coating porosity decreased. This was attributed to the fact that a small amount of PVA leads to improved stabilization of coating components.
3. The use of cobinders increased the elastic property of the coating colors, except when the coating colors contained small amounts of PVA. This was attributed to the fact that flocculation of the coating components increases with the addition of a cobinder.
4. Two types of flocculation mechanisms were proposed. For PVA as a cobinder, PVA serves as a stabilizing agent after adsorbing onto the pigment surface at low dosages. When larger amounts of PVA are used, the gelling of coating components by a linear polyvinyl alcohol polymer prevails; this gelling increases the viscosity and elastic properties as well as the coating porosity.
5. The viscosity results showed that CMC colors have less tenacious flocculation properties as compared to PVA colors. For CMC as a cobinder, CMC molecules remaining in the aqueous phase flocculate the pigment via a depletion flocculation mechanism. The depletion flocculation by CMC was more evident in platy clay coating colors.

ACKNOWLEDGMENTS

The authors are grateful for the support of the Ministry of Education, Science and Technology, MEST in the Rep. Korea, Grant No. 2009-0080016.

REFERENCES CITED

- Al-Turaif, H., Bousfield, D. W., and LePoutre, P. (2002). "The influence of substrate absorbency on coating surface chemistry," *Progress in Organic Coatings*, 44, 307-315. DOI: 10.1016/S0300-9440(02)00071-1
- Bohnenkamp, B., Tietz, M., and Trefz, M. (2005). "New development results of curtain coatings for various paper grades," *Proceedings of TAPPI Coating Conference*
- Dahlvik, P., Choi, K. Y., Jeon, I. S., Koo, B. H. and Bluvol, G. (2012). "First commercial curtain coater application for wood-free paper grades," *Proceedings of TAPPI PaperCon Conference*, TAPPI Press, Atlanta.
- Endres, I., and Tietz, M. (2007). "Blade, film, and curtain coating techniques and their influence on paper surface characteristics," *TAPPI J.* 6(11), 24-32.
- Fadat, G., Engström, G., and Rigdahl, M. (1988). "The effect of dissolved polymers on the rheological properties of coating colours," *Rheol. Acta* 27, 289-297. DOI: 10.1007/BF01329745
- Fröhlich, U., and Tietz, M. (2004). "Influence of surfactants on curtain coater runnability and paper quality," *Proceedings of TAPPI Coating Conference*
- Işçi, S., Ünlü, C. H., Atici, O., and Güngör, N. (2006). "Rheology and structure of aqueous bentonite – polyvinyl alcohol dispersions," *Bull. Mater. Sci.* 29(5), 449-456. DOI: 10.1007/BF02914075
- Kim, C. H., Youn, H. J., and Lee, H. L. (2013). "Characterization of the pore structure and clay orientation in curtain coating layers using SEM and image analysis," *TAPPI J.* 12(8), 31-39.
- Kistler, S.F. (1983). "The fluid mechanics of curtain coating and related viscous surface flows with contact lines," *Ph.D. thesis, University of Minnesota, Minneapolis.*
- Klass, C. P. (2004). "Is curtain coating ready for prime time?," *Solutions*, December, 31-32.
- Lee, H. L., Kim, J. D., Lee, K. H., Kim, C. H., and Youn, H. J. (2012). "Effect of coating formulations and drying methods on the coverage and smoothness of brown grade base papers," *Nordic Pulp Paper Res. J.* 27(1), 79-85. DOI: 10.3183/NPPRJ-2012-27-01-p079-085
- Lepoutre, P. (1989). "The structure of paper coatings: an update," TAPPI Press, Atlanta, GA.
- Mendez, B., and Morita, H. (2001). "Curtain coating – A novel coating techniques for high-precision coating," *Wochenblatt fuer Papierfabrikation* 129(22), 1492-1497.
- Nisogi, H., Bousfield, D. W., and Lepoutre, P. F. (2000). "Influence of coating rheology on final coating properties," *TAPPI J.* 83(2), 100-106.
- Renvall, S., Nurmiainen, T., Haavisto, J., Kim, J. D., Endres, I., Urscheler, R., Park, K. J., and Salminen, P. J. (2009). "White top liner with on-machine multilayer curtain coating – Part 1 Technology development and Part 2 Mill experiences," *Proceedings of PTS Symposium*

- Sandas, S. E., and Salminen, P. J. (1991). "Pigment-cobinder interactions and their impact on coating rheology, dewatering, and performance," *TAPPI J.* 74(12), 179-187.
- Sjöberg, M., Bergström, L., Larsson, A., and Sjöström, E. (1999). "The effect of polymer and surfactant adsorption on the colloidal stability and rheology of kaolin dispersions," *Colloids Surf. A* 159, 197-208. DOI: 10.1016/S0927-7757(99)00174-0
- Tadros, D. T. F. (1996). "Correlation of viscoelastic properties of stable and flocculated suspensions with their interparticle interactions," *Adv. Colloid Interface Sci.* 68, 97.
- Tadros, T. (2007) "Colloid stability: The role of surface forces, Part I," in: Tadros, T. F. (ed.), *Colloids & Surface Sci.* 1, 1-22. DOI: 10.1016/S0001-8686(96)00305-3
- Theng, B. K. G. (1982). "Clay-polymer interactions: Summary and perspectives," *Clays Clay Miner.* 30(1), 1-10. DOI: 10.1346/CCMN.1982.0300101
- Trefz, M., and Fröhlich, U. (2005). "Production experience with curtain coating for wood-free coated paper," *TAPPI J.* 4(11), 3-7.
- Triantafillopoulos, N., Grön, J., Luostarinen, I., and Paloviita, P. (2004a). "Operational issues in high-speed curtain coating of paper, Part 1: The principles of curtain coating," *TAPPI J.* 3(11), 6-10.
- Triantafillopoulos, N., Grön, J., Luostarinen, I., and Paloviita, P. (2004b). "Operational issues in high-speed curtain coating of paper, Part 2: Curtain coating of lightweight coated paper," *TAPPI J.* 3(12), 11-16.
- Urscheler, R., Roper, J., Dobler, F., and Haavisto, J. (2006). "Multilayer curtain coating: An enabling method for new paper functions," *Proceedings of TAPPI Coating Conference*
- Whalen-Shaw, M., and Gautam, N. (1990). "A model for the colloidal and rheological characteristics of clay, latex, and CMC formulations," *Proceedings of TAPPI Coating Conference*, TAPPI Press, Atlanta.

Article submitted: January 23, 2015; Peer review completed: April 19, 2015; Revised version received: May 21, 2015; Accepted: July 3, 2015; Published: September 4, 2015. DOI: 10.15376/biores.10.4.7188-7202